Corresponding Author: Dr. mehdi salehifar, PhD

Corresponding Author's Institution: Electronic Engineering department

First Author: mehdi salehifar

Order of Authors: mehdi salehifar; Manuel Moreno Eguilaz; ghanim putrus; peter barras; Ramin Salehi Arashloo

Abstract: Multiphase brushless direct current (BLDC) motors can meet the increasing demand for higher reliability in motor drives applicable in electric vehicles by integrating fault diagnosis to a fault-tolerant (FT) control method. To achieve this goal, a modified FT finite control set model predictive control (FCS-MPC) is proposed in this paper. The dead beat control is used to predict the reference voltage applied by inverter. A sensitivity analysis is done to show effect of model uncertainty on controller performance. In addition, a simple, fast and general open switch and short circuit fault detection (FD) method in voltage source inverter (VSI) is presented. The FD method is capable of detecting open switch, open phase, and short circuit faults without any auxiliary variable. Moreover, it is robust to both speed and load transients in motor drive. To validate the presented theory, experimental results are conducted on a five-phase BLDC motor drive with rotor router in wheel structure.

Cover Letter

Simplified Fault Tolerant Finite Control Set Model Predictive Control of Five-Phase Inverter Supplying PM Motor in Electric Vehicle Drive

Mehdi SALEHIFAR, Manuel MORENO-EGUILAZ, G. PUTRUS, P. BARRAS, Ramin SALEHI ARASHLOO

Theoretical Foundation

Due to high reliability requirements in electric vehicles, fault-tolerant multiphase permanent magnet (PM) motor drives are aging more interest for application in this area. A simple, fast, and robust control method should be used to control the motor. Model predictive controllers are among one of the best methods capable of achieving aforementioned characteristics. On the other side to maintain continuous operation of the motor, it is necessary to detect and isolate fault in real time. After that, system hardware and control method can be reconfigured according to the new conditions.

In this paper, a modified finite control set model predictive control is developed to control a five-phase PM motor under healthy, one faulty phase, and two-adjacent faulty phase mode. In addition, assuming faults in the voltage source inverter supplying the motor, a simple open switch and single switch short circuit fault diagnosis method is proposed. Therefore, by integrating fault diagnosis method to control algorithm, a continuous operation of motor drive is achieved. Theory of fault detection method, and fault tolerant control strategy is explained. In order to validate the theory, experimental results are conducted on a five-phase PM motor drive setup.

Work Originality Confirmation

The results presented in this paper are original and have not been previously published by other authors.

Simplified Fault Tolerant Finite Control Set Model Predictive Control of a Five-Phase Inverter Supplying BLDC Motor in Electric Vehicle Drive

Mehdi SALEHIFAR[1], Manuel MORENO-EGUILAZ[2], G. PUTRUS[3], P. BARRAS[4], Ramin SALEHI ARASHLOO[5]

[1]CORRESPONDING AUTHOR, mehdi.salehifar@mcia.upc.edu

[2]manuel.moreno.eguilaz@upc.edu

[3]ghanim.putrus@northumbria.ac.uk

[4]peter.barras@sevcon.com

[5]ramin.salehi@mcia.upc.edu

M. Salehifar, M. Moreno and R. Salehi are with Electronic Engineering Department, UPC, Rambla Sant Nebridi, 22, Terrassa, Spain,

Tel: +34 678132937

Fax: +34 937398972

M. Salehifar, and G. Putrus are with Physics and Engineering Department, Northumbria University, Newcastle, UK, NE1 8ST.

P. Barras is with Sevcon LTD, Newcastle, UK NE11 0QA.

Abstract – Multiphase brushless direct current (BLDC) motors can meet the increasing demand for higher reliability in motor drives applicable in electric vehicles by integrating fault diagnosis to a fault-tolerant (FT) control method. To achieve this goal, a modified FT finite control set model predictive control (FCS-MPC) is proposed in this paper. The dead beat control is used to predict the reference

voltage applied by inverter. A sensitivity analysis is done to show effect of model uncertainty on controller performance. In addition, a simple, fast and general open switch and short circuit fault detection (FD) method in voltage source inverter (VSI) is presented. The FD method is capable of detecting open switch, open phase, and short circuit faults without any auxiliary variable. Moreover, it is robust to both speed and load transients in motor drive. To validate the presented theory, experimental results are conducted on a five-phase BLDC motor drive with rotor router in wheel structure.

1. Introduction

Achieving high reliability is a new trend established in the growing industry of electric vehicles. Others sectors such as renewable energy are imposing the same trend as well [1]. Redundancy and FT design are two main solutions to gain high reliability. Due to its lower cost and smaller space requirements, a FT design is dominantly accepted for industrial applications such as motor drives. More electric aircraft, renewable energy, and transportation are other application areas for FT drives. Regarding motor drives applicable in electric and hybrid electric vehicles, multiphase BLDC motors can achieve high reliability due to their FT capability [2], [3], [4].

A multiphase FT converter should be used to supply the motor. The converter is subjected to open switch and short circuit faults. So, a FT converter should be used. It means that a reconfigurable control with an included FD strategy has to be implemented.

Faults and corresponding FD methods in VSIs have been thoroughly investigated in the literature [5]. The fault types in a VSI can be either open switch faults or short circuit faults. Performance of the motor drive is reduced due to the open switch fault. To maintain the continuous operation of the motor drive, it is necessary to detect and isolate the fault in a short interval of time. On the other side, a short circuit fault should be detected and isolated very fast. Otherwise, the system will shut down. Proposed

FD methods in literature mainly study only one type of fault (i.e. either short circuit fault [6] or open switch fault [7]). Therefore, there is a lack of research on FD methods for both fault types at the same time.

Several FD algorithms have been investigated in literature. However, application area is mainly the three-phase energy conversion systems [8]-[10]. There is lack of knowledge on FD methods in VSI supplying multiphase motor drives.

On the other side, presented methods have addressed either FD methods or FT control methods [11-13]. Therefore, it is necessary to introduce FT control methods capable of generating fault alarms due to a fault in VSI.

By utilizing powerful digital microprocessors, predictive control methods are gaining more attention for industrial applications in recent years. MPC methods presented in literature can be categorized in two categories: deadbeat control, and FCS-MPC [14]. Regarding deadbeat control method, a machine model is used to calculate the reference voltages, so that motor phase current is able to follow the reference current [15], [16]. Predictive deadbeat control is used in [17] to implement FT control of a five-phase BLDC machine under healthy and faulty conditions; a sensitivity analysis has been done on the control method. An improved predictive deadbeat control of five-phase BLDC machine has been presented in [18]; in contrast to presented method in [17], authors use extended Kalman filter to predict the motor phase currents; robustness to the nonlinearly of the inverter, and non-ideal model parameters are the main advantages of this method. This method has a high computational cost. A deadbeat power control is presented in [19] to improve the steady-state and transient response of PWM rectifier under unbalanced grid conditions. To further improve the controller performance, calculation delay is compensated. A new deadbeat controller based on feedback and feed forward linearization is presented in [20]; this method has a high dynamic response, at the same time it is robust to parameter uncertainties and disturbances.

Regarding FCS-MPC, using a motor model, the stator current is predicted at the end of next switching vector using all possible switching vectors of the inverter. After that, a cost function is calculated from

difference between the reference and predicted current. The switching vector associated with the minimum cost is chosen as the optimal switching vector for next switching step [21].

Among predictive control methods, FCS-MPC is a simple, flexible, fast method, and robust to parameter uncertainty in comparison to other methods [21], [22], [23].

Another important characteristic of the control and fault diagnosis method in case of a multiphase motor drive is simple reconfiguration. In case of a five-phase BLDC motor, it can be operated with a five-phase, four-phase or three-phase inverter. Consequently, FD and control method should work under each configuration.

To overcome the aforementioned limitations in literature, a simplified version of the conventional FCS-MPC is developed in this paper to control a two-level VSI supplying a five-phase BLDC motor. This method has the advantage of less computational cost. Furthermore, it can be easily reconfigured in case of a fault in inverter. This is the first contribution of this paper.

On the other side, by taking advantage of signals provided by the control method, a simple and robust open switch and short circuit FD method is developed in this paper. An observer is used to localize the faulty components. This method is cost effective since no extra sensor is necessary to implement the control method. This is the second contribution of this paper.

The rest of this paper is organized as follows. The dynamic model of the motor drive and control method are discussed in section 2. The proposed FD method is presented in section 3. A sensitivity analysis on controller performance is presented in section 4. To validate the theory, experimental results on the FT control algorithm and FD method are shown in section 5. The conclusions of this paper are discussed in section 6.

2. Fault Tolerant Control of the Five-phase BLDC Motor Drive

The dynamic model of a five-phase BLDC motor is briefly discussed in this section. The system under study is shown in Fig. 1. As it can be seen, a five-phase BLDC motor is supplied by a five-phase inverter; a TRIAC switch is used in each phase of the motor in order to isolate the faulty phase. It should be noted that there is a voltage drop on TRIAC under all operating conditions of the motor;

consequently the maximum available voltage is reduced. This design limit should be considered in design of practical motor drive systems working in field-weakening region.

HERE FIG. 1

The model of a five-phase BLDC motor with trapezoidal back electro motive force (EMF) under healthy mode is as:

$$
\begin{bmatrix} v_{ax} - e_a \\ v_{bx} - e_b \\ v_{cx} - e_c \\ v_{dx} - e_d \\ v_{ex} - e_e \end{bmatrix} = \begin{bmatrix} r_a & 0 & 0 & 0 & 0 \\ 0 & r_b & 0 & 0 & 0 \\ 0 & 0 & r_c & 0 & 0 \\ 0 & 0 & 0 & r_d & 0 \\ 0 & 0 & 0 & 0 & r_e \end{bmatrix} \begin{bmatrix} i_a \\ i_b \\ i_c \\ i_d \\ i_e \end{bmatrix} + \begin{bmatrix} l_a & m_1 & m_2 & m_2 & m_1 \\ m_1 & l_b & m_1 & m_2 & m_2 \\ m_2 & m_1 & l_c & m_1 & m_2 \\ m_2 & m_2 & m_1 & l_d & m_1 \\ m_1 & m_2 & m_2 & m_1 & l_e \end{bmatrix} \frac{d}{dt} \begin{bmatrix} i_a \\ i_b \\ i_c \\ i_d \\ i_e \end{bmatrix}.
\tag{1}
$$

where i_j is the phase current, v_{jx} is the phase to neutral voltage of each phase, r_j is the phase equivalent resistance, l_j is the phase equivalent inductance, m_1 is mutual inductance between two-adjacent phase, m_2 is mutual inductance between two-nonadjacent phase, e_j is the back EMF in each phase of the motor where j={a, b, c, d, e}. The back EMF will be estimated as follows:

$$
\begin{aligned}
e &= \lambda_{m1} \omega_e \cos(\theta - \frac{2\pi n}{5}) \\
&+ \lambda_{m3} 3\omega_e \cos(3(\theta - \frac{2\pi n}{5})), \ n = 0,1,2,3,4.
\end{aligned}
\tag{2}
$$

where λ_{m1} and λ_{m3} are the first and third harmonic amplitudes of the rotor flux linkage; ω_e is the electrical rotational velocity, Θ is the rotor electrical angle, and $n=0,1,2,3,4$ represents phase a, b, c, d, e, respectively.

2.1 Model of the Motor under Faulty Mode

Under an open phase fault, neutral voltage of the motor floats due to the back EMF in the faulty phase [24], [25]. So, the same healthy model of the motor in (1) can be used in faulty mode if the induced voltage in healthy phases is considered. This voltage is shown by v_n in this paper and its value is calculated similarly to [25].

Under faulty condition, the row and column related to the faulty phase can be removed from (1). The machine model under one faulty phase A is therefore modified as:

$$\begin{bmatrix} v_{bx} - e_b \\ v_{cx} - e_c \\ v_{dx} - e_d \\ v_{ex} - e_e \end{bmatrix} = \begin{bmatrix} r_b & 0 & 0 & 0 \\ 0 & r_c & 0 & 0 \\ 0 & 0 & r_d & 0 \\ 0 & 0 & 0 & r_e \end{bmatrix} \begin{bmatrix} i_b \\ i_c \\ i_d \\ i_e \end{bmatrix} + \begin{bmatrix} l_b & m_1 & m_2 & m_2 \\ m_1 & l_c & m_1 & m_2 \\ m_2 & m_1 & l_d & m_1 \\ m_2 & m_2 & m_1 & l_e \end{bmatrix} \frac{d}{dt} \begin{bmatrix} i_b \\ i_c \\ i_d \\ i_e \end{bmatrix} - v_n \begin{bmatrix} 1 \\ 1 \\ 1 \\ 1 \end{bmatrix}. \tag{3}$$

$$v_n = \frac{m_1}{4} \left(\frac{di_b}{dt} + \frac{di_e}{dt} \right) + \frac{m_2}{4} \left(\frac{di_c}{dt} + \frac{di_d}{dt} \right).$$

Similarly, in case of open circuit fault in both phases *A* and *B*, the model is recalculated as:

$$\begin{bmatrix} v_{cx} - e_c \\ v_{dx} - e_d \\ v_{ex} - e_e \end{bmatrix} = \begin{bmatrix} r_c & 0 & 0 \\ 0 & r_d & 0 \\ 0 & 0 & r_e \end{bmatrix} \begin{bmatrix} i_c \\ i_d \\ i_e \end{bmatrix} + \begin{bmatrix} l_c & m_1 & m_2 \\ m_1 & l_d & m_1 \\ m_2 & m_1 & l_e \end{bmatrix} \frac{d}{dt} \begin{bmatrix} i_c \\ i_d \\ i_e \end{bmatrix} - v_n \begin{bmatrix} 1 \\ 1 \\ 1 \end{bmatrix}. \tag{4}$$

$$v_n = \frac{(m_1 + m_2)}{3} \frac{di_c}{dt} + \frac{2}{3} m_2 \frac{di_d}{dt} + \frac{(m_1 + m_2)}{3} \frac{di_e}{dt}.$$

The nominal model of the motor without considering disturbance and parameter uncertainties can be rewritten from (1) as:

$$\dot{x} = Ax + Bu, \tag{5}$$

$$\mathbf{x} = [i_a \ i_b \ i_c \ i_d \ i_e]^T,$$

$$\mathbf{u} = [v_{ax} - e_a \ v_{bx} - e_b \ v_{cx} - e_c \ v_{dx} - e_d \ v_{ex} - e_e]^T.$$

where **A=-R/L**, and **B=1/L**, **R** and **L** are resistance and inductance matrixes of the machine, respectively.

2.2 Fault-Tolerant FCS-MPC of a Five-Phase PM Motor

In this section, the theory of the control method is explained. The control method (i.e. FCS-MPC) of the VSI can be done in two different ways. According to the first method, the phase currents of the motor are predicted using the motor model and previous switching command for all possible space vectors in the VSI. The BLDC motor in system under study is supplied by a five phase, four-phase, and three-phase inverter under healthy, one faulty phase, and two-faulty phase mode, respectively. Control method should be reconfigured under each operating mode. The number of current predictions is equal to 32 in case of a five-phase inverter, equal to 16 in case of a four-phase inverter and equal to 8 in case of a three-phase inverter. The theory in case of the four-phase inverter has been presented in [26].

According to this method, a cost function is defined as the difference between the predicted current and the reference current. The switching vector that produces the minimum cost is chosen as the optimal switching vector and applied to the inverter during the next switching sample. This method is simple and effective; however, its computational cost is high.

To reduce number of calculations in the conventional FCS-MPC, a simplified of FCS-MPC has been presented in [27], and [28], recently. According to this method, in the first step, the equivalent reference voltage to maintain the reference current by the inverter is predicted. After that, the closest switching vector to the reference voltage is chosen and applied to the inverter during the next sampling time. This method is chosen for this paper; it is applied to a two-level five-phase inverter supplying a BLDC motor. Theory of the control method is explained in the following.

Similar to the deadbeat control algorithm, the motor model is used to predict the reference voltages. The necessary voltage to track the reference current (i.e. x^*) at the next switching period can be calculated in discrete form as:

$$U_{eq}(k+1) = B^{-1}((x^*(k+1) - x(k)) \times T_{samp}^{-1} - Ax(k+1)).$$

(6)

where T_{samp} is the switching period.

Similar to [29], a fourth-order Lagrange extrapolation is used to predict the reference current at time k+1 as:

$$x^*(k+1) = 4x^*(k) - 6x^*(k-1) + 4x^*(k-2) - x^*(k-3)$$

(7)

In practice, performance of the predictive controller is affected by delay due to calculation in the digital signal processor, gate drivers, and non-ideal switches [20], [27]. Delay due to computational time is the most important parameter [20]. This delay can be compensated by calculating the reference voltage so that the current at the end of next sampling period (i.e. $i(k+2)$) is equal to the reference current. Therefore, it is possible to do computations during the current sampling period without affecting the controller performance.

In order to compensate the delay, in the first step, the phase current of the motor at the end of the current switching step is predicted from (5) as:

$$x(k+1) = T_{samp} \times (Ax(x) + Bu(k)) + x(k) \tag{8}$$

In the second step, the reference voltage is calculated as:

$$U_{eq}(k+1) = B^{-1}((x^*(k+2) - x(k+1)) \times T_{samp}^{-1} - Ax(k+1)). \tag{9}$$

Similar to (7), the reference current at time k+2 is predicted as:

$$x^*(k+2) = 4x^*(k+1) - 6x^*(k) + 4x^*(k-1) - x^*(k-2) \tag{10}$$

The calculated reference voltages in (9) are transferred to the stationary reference frame as:

$$\begin{bmatrix} v_\alpha^{ref} \\ v_\beta^{ref} \\ v_x^{ref} \\ v_y^{ref} \\ v_o^{ref} \end{bmatrix} = T \begin{bmatrix} v_a^{ref} \\ v_b^{ref} \\ v_c^{ref} \\ v_d^{ref} \\ v_e^{ref} \end{bmatrix} \tag{11}$$

where T is the Fortescue transformation.

In the next step, the closest switching vector to the reference vector among the possible vectors of a five-phase inverter (i.e. 32 possible vectors) is determined. This vector is applied during the next switching period. To achieve this goal, the cost function for each switching vector is calculated as:

$$\begin{aligned} g_{5ph} &= (v_\alpha^{ref} - v_\alpha)^2 + (v_\beta^{ref} - v_\beta)^2 + \\ &\quad (v_x^{ref} - v_x)^2 + (v_y^{ref} - v_y)^2 \end{aligned} \tag{12}$$

This method requires heavy computation. To overcome this problem, four of the closest switching vectors to the reference vector can be found. Therefore, the cost function calculation can be reduced to 4 non-zero vectors plus two zero vectors in case of a five-phase inverter.

The proposed strategy in [30] is used in this paper to find the closest switching vectors to the reference vector. In the first step, the elements of reference voltage v_{ref} are sorted in a descending order using permutation matrix **P**. In the second step, displaced switching vectors v_{dj} are obtained by multiplying $\mathbf{P^T}$ and upper triangular matrix **D** as shown in (13).

$$\hat{\mathbf{D}} = \begin{bmatrix} 1 & 1 & 1 & \dots & 1 \\ 0 & 1 & 1 & \dots & 1 \\ 0 & 0 & 1 & \dots & 1 \\ & & \dots & & \\ & & & \dots & 1 \end{bmatrix}, \quad \mathbf{D} = \mathbf{P^T}\hat{\mathbf{D}} \tag{13}$$

where $\mathbf{P^T}$ is the transpose matrix of $\mathbf{P}$.

In the second step, the cost function in (12) is calculated for six vectors in (13). Finally, the switching vector with the minimum cost function is chosen and applied during the next switching period.

Under faulty mode, inverter is reconfigured to a four-phase in case of one faulty phase and a three-phase inverter in case of two-faulty phase mode. The principal of control method is similar to the five-phase inverter. However, the motor model and switching vectors are adapted according to the inverter topology.

3. Fault Diagnostic Method

In order to diagnose a fault in an inverter, a simple FD method is presented in this paper. The cost function value in (12) is increased significantly in case of a fault in inverter. This advantage is used to generate a fault alarm as:

$$\text{Fault Alarm} = \begin{cases} \text{Fault} & g > \text{Th} \\ \text{Healthy} & g < \text{Th} \end{cases} \tag{14}$$

where Th is a threshold value to distinguish the healthy mode from the faulty mode.

To determine the threshold value under healthy condition, the switching vectors of a five-phase inverter are shown in Fig. 2. As it can be seen, the α-β plane is divided to three parts including A, B, and C. At each part, the closest vector to the reference vector is chosen and applied to the inverter during the next switching period. The maximum distance between the reference vector and the closest switching vector is shown in points A, and B at α-β and x-y planes. If the closest vector is considered (1101) and reference vector is at point A, the cost function in (12) is equal to $0.081 \times V_{dc}$. This value is the highest theoretical difference between the reference vector and the closest cost function. It should be noted that under the healthy operation of the machine, the reference vector in x-y plane is negligible in comparison to α-β plane. As a result, the threshold value in (14) should be chosen higher than $0.081 \times V_{dc}$ to avoid false alarms.

HERE FIG. 2

If the cost function is higher than the threshold value, a fault alarm is generated. After that, an observer is used to localize the faulty component. The FD method is cost effective, since no extra hardware is used to localize the faulty switch.

In order to localize to faulty switch, a simple proportional-integral observer is designed in this paper to predict the phase currents of the motor. Inputs of the observer are the output voltages of the control method. If the mutual inductances in (1) are considered negligible, the observer is designed as:

$$
\begin{bmatrix} L_a & -L_b & 0 & 0 \\ 0 & L_b & -L_c & 0 \\ 0 & 0 & L_c & -L_d \\ L_e & L_e & L_e & L_e+L_d \end{bmatrix} \frac{d}{dt} \begin{bmatrix} \hat{i}_a \\ \hat{i}_b \\ \hat{i}_c \\ \hat{i}_d \end{bmatrix} = \begin{bmatrix} v_{ab} - e_{ab} \\ v_{bc} - e_{bc} \\ v_{cd} - e_{cd} \\ v_{de} - e_{de} \end{bmatrix} -
$$
$$
\begin{bmatrix} R_a - R_b & 0 & 0 \\ 0 & R_b - R_c & 0 \\ 0 & 0 & R_c & -R_d \\ R_e & R_e & R_e & R_d + R_e \end{bmatrix} \begin{bmatrix} \hat{i}_a \\ \hat{i}_b \\ \hat{i}_c \\ \hat{i}_d \end{bmatrix} - F(\begin{bmatrix} \delta_a \\ \delta_b \\ \delta_c \\ \delta_d \end{bmatrix}).
$$

$$(15)$$

where δ is the error between estimated and real current, and F is a nonlinear proportional-integrator function in discrete form as follows:

$$F(z) = K_p + K_i \frac{T_s}{Z-1} \tag{16}$$

where K_p and K_i are the proportional and integral coefficients, respectively and T_s is the sampling period.

The output of F function is called the residue value as follows:

$$s = F(z). \tag{17}$$

The residue value calculated in (17) is used to localize the faulty leg as follows:

$$FD = \max(|s|). \tag{18}$$

According to (18), the faulty phase has the highest s value among others. Then faulty switch in the faulty leg can be determined from the sign of s as follows:

$$sign(s) = \begin{cases} >0 & upper\ open\ switch\ fault \\ <0 & lower\ open\ switch\ fault \end{cases}. \tag{19}$$

In case of a short circuit fault, the faulty components are localized as:

$$sign(s) = \begin{cases} < 0 & upper\ short\ switch\ fault \\ > 0 & lower\ short\ switch\ fault \end{cases}.$$ (20)

From (19) and (20), the faulty component can be localized according to table I.

HERE Table. I

Under an open phase fault, the faulty phase current is reduced to zero whereas in case of the short circuit fault, the phase current is different than zero. This advantage can be used to distinguish the open switch from the short circuit fault.

In case of a shoot through in one leg of the inverter, the whole system may shutdown. The main concern under this condition is to detect and isolate the faulty leg. It should be noted that modern gate drives are able to detect this fault. Therefore, the feedback from the gate driver can be sent to the proposed FT control algorithm to isolate the faulty leg and maintain continuous operation of the motor.

It should be noted that there are conditions where the semiconductors are neither open nor short circuit. If the phase current under this mode is zero while the reference current is none zero, this can lead to a false alarm. The proposed FD method identifies this case as an open switch fault. To avoid false alarm, additional hardware based methods can be used to effectively manage this condition.

The isolation method of a faulty phase is another important design criterion in a FT system. After the open phase fault, the gate signal of the faulty leg is removed and phase current can be disconnected by a static switch such as a TRIAC. In case of the short circuit fault, the phase current is no longer near zero after the fault. Therefore, the isolation method is more complicated. Under this condition, at the first step, the gate signal of all healthy phases is removed. When current value in the faulty phase is reduced to zero, the TRIAC switch is turned off to isolate the faulty phase. In the next step, the drive setup can be reconfigured and initiated according to the new configuration of the inverter.

The fault-tolerant control (FTC) algorithm of the five-phase BLDC motor drive and the FD block diagram are shown in Fig. 3. As it can be seen, a fault code (i.e. FC) is generated by the FD block. After that, the control algorithm is reconfigured according to this code.

HERE FIG. 3

4. Sensitivity Analysis

According to the proposed control method, the machine model in (1) is used to predict the reference voltage similar to the predictive deadbeat control method. Therefore, the performance of the FCS-MPC is affected by parameter uncertainties. This issue is analyzed in detail in the following.

The behavior of the control method can be affected in different ways. The inaccurate value of dc-link voltage, nonlinear behavior of the switch (i.e. voltage drop on switch and switching dead time), and inaccuracy in parameters of the motor model are the most important ones among others. Each case is briefly discussed here.

The error in dc-link voltage measurement, the error due to non-linear inverter caused by switching dead time and voltage drop on switches, and error in the estimated back EMF can be modelled as:

$$u(k) = u(k)_{nom} + \Delta u(k) \tag{21}$$

where $\Delta u(k)$ is the modelled voltage error and $u(k)_{nom}$ is the ideal input. Since after, all ideal variables are shown with lower case x_{nom}.

Similarly, error in the stator phase resistance and self-inductance can be modelled as:

$$A = A_{nom} + \Delta A \tag{22}$$

$$B = B_{nom} + \Delta B \tag{23}$$

where ΔA and ΔB are the error in phase resistance, and self-inductance, respectively.

The current prediction is rewritten in presence of the uncertain parameters by replacing (21)-(23) in (8) as follows:

$$\begin{aligned} x(k+1) &= T_{samp} \times ((A + \Delta A)x(k) + Bu(k)) + x(k) \\ &= x(k+1)_{nom} + \Delta x(k+1) \end{aligned} \tag{24}$$

$$\begin{aligned} x(k+1) &= T_{samp} \times (Ax(k) + B(u(k) + \Delta u(k))) + x(k) \\ &= x(k+1)_{nom} + \Delta x(k+1) \end{aligned} \tag{25}$$

$$\begin{aligned} x(k+1) &= T_{samp} \times (Ax(k) + (B + \Delta B)u(k)) + x(k) \\ &= x(k+1)_{nom} + \Delta x(k+1) \end{aligned} \tag{26}$$

By replacing (24)-(26) in (9), the equivalent voltage control under non-ideal condition is calculated as follows:

$$U_{eq} = B^{-1}((x*(k+2) - x(k+1) - \Delta x(k+1)) \times T_{samp}^{-1} - (A + \Delta A)(x(k+1) + \Delta x(k+1)))$$
$$= U_{eq-nom} - T_{samp}^{-1} B^{-1} \Delta x(k+1) \times (1 + T_{samp} \times (A + \Delta A)) - B^{-1} \Delta A x(k+1) \tag{27}$$

$$U_{eq} = (B + \Delta B)^{-1}((x*(k+2) - x(k+1) - \Delta x(k+1)) \times T_{samp}^{-1} - A(x(k+1) + \Delta x(k+1)))$$
$$= U_{eq-nom} - \Delta B / B \times B^{-1}((x*(k+2) - x(k+1)) \times T_{samp}^{-1} - A x(k+1)) \tag{28}$$
$$- T_{samp}^{-1} B^{-1} (1 - \Delta B / B) \Delta x(k+1) \times (1 + T_{samp} \times A) - B^{-1} \Delta A x(k+1)$$

$$U_{eq} = B^{-1}(((x*(k+2) - x(k+1) - \Delta x(k+1)) T_{samp}^{-1} - A(x(k+1) + \Delta x(k+1))))$$
$$= U_{eq-nom} - T_{samp}^{-1} B^{-1} \Delta x(k+1) \times (1 + T_{samp} \times A) \tag{29}$$

Equivalent voltages in (27)-(29) can be further simplified as:

$$U_{eq} = U_{eq-nom} - B^{-1} \Delta A(x(k) \times (1 + T_{samp} \times (A + \Delta A)) + \Delta A x(k+1)) \tag{30}$$

$$U_{eq} = U_{eq-nom}(1 - \Delta B / B) - B^{-1} \Delta B(1 - \Delta B / B) u(k) \times (1 + T_{samp} \times A) \tag{31}$$

$$U_{eq} = U_{eq-nom} - \Delta u(k) \times (1 + T_{samp} \times A) \tag{32}$$

As it can be seen in (30)-(32), the non-ideal voltage value can be decreased by reducing the sampling period. On the other hand, higher absolute value of the parameters and dc-link voltage error can cause higher error. According to (31), if the error value in the phase self-inductance is equal to 100 % of the real value, the controller becomes unstable.

In the following section, simulations are conducted to study the effects of the uncertainty on controller performance. To study the effect of parameter uncertainty, several tests are considered according to table II. For each case, the energy of the error is calculated as follows:

$$E = \int (i_a^* - i_a)^2 + (i_b^* - i_b)^2 + (i_c^* - i_c)^2 + (i_d^* - i_d)^2 + (i_e^* - i_e)^2 \, dt. \tag{33}$$

The motor parameters in simulation model are according to table III. The dc-link voltage of inverter is 24 V, switching frequency is 20 kHz, and motor speed is set at 50 rpm.

Under each operating mode, the phase current in per-unit, derivative of the phase current normalized with respect to the healthy phase, and the energy of the error are calculated. The final results are shown in Fig. 4 under normal, one-faulty phase, two-adjacent faulty phase, and two-non-adjacent faulty phase mode. According to Fig. 4, inverter non-linear parameters can result in a high error. The inverter non-linearity causes the highest error. Result under two-faulty phase condition are shown in Figs. 4(c) and

4(d). As it can be seen, the over estimation of the self-inductance has a higher impact on accuracy of control method. From Fig. 4, the energy of the error under faulty mode in most cases is higher than the normal mode operation. Furthermore, the symmetrical waveforms and slower dynamics are the main reasons for lower error under normal mode operation.

HERE Table. II

HERE Table. III

HERE FIG. 4

5. Experimental Results

In order to validate the developed theory, experimental results are provided on a laboratory setup as shown in Fig. 5. The setup has been designed to study traction motor drives applicable in the electric vehicles.

HERE FIG. 5

A five-phase BLDC motor with an outer rotor in wheel structure is coupled to a three-phase PMSM drive as load motor. The load motor is supplied with a Siemens commercial drive. The parameters of the five-phase motor are given in Table III. This motor is supplied with a two-level five-phase inverter; the DC-link voltage is 24 V. The IGBT SKM75GB12T4 model is used in inverter. The Skyper32 gate drivers from Semikron are used to control IGBT switches. Short circuit protection is done by sensing the Collector-Emitter voltage when IGBT is on. Also, the gate driver can be set so that it never allows the second IGBT in the same leg is turned on while other switch is still on. This protection mechanism is so effective to avoid shoot through. In addition, a feedback signal is generated by the gate driver after short circuit FD. Therefore, the FT controller can isolate the faulty leg and reconfigure the whole drive after receiving the fault feedback from gate driver IC.

The phase currents are measured by Hall-Effect sensors. The measured currents are sent to a dSPACE control board, model ds1005. The sampling frequency is 5 kHz.

The control algorithm is implemented in dSPACE according to the field oriented control strategy as shown in Fig. 3. In this paper, the focus is on the inner control loop. The optimized reference currents of

the motor under healthy and faulty conditions have been extensively studied in literature. The calculated currents in [14] are used in this paper as the optimal reference currents. The FCS-MPC should track these currents under each operational mode of the motor.

The experimental results are shown in two sections. In the first part, different fault types and operating scenarios are studied. In the second step, the continuous operation of the motor drive in presence of a fault is demonstrated.

5.1. Experimental Results of Fault Detection

In this first part, the robustness of the FD method to the load transients is evaluated. Two load step changes equal to 50 % are forced on the motor phase currents. Experimental waveforms of the phase currents and the cost function are shown in Fig. 6(a). As it can be seen, the proposed FD method is robust to the load transients.

A high performance FD method should be robust to the common operational modes in an electric vehicle such as acceleration, deceleration, and reverse operating mode. Therefore, each one of these modes was applied to the setup. Waveforms for each case are shown in Figs. 6(c)-6(d). As it can be seen, the proposed method is robust to these conditions.

HERE FIG. 6

In the third step, different open circuit fault types are forced on the inverter by removing the gate signal of the IGBT. A single switch fault is forced in phase A. Experimental waveforms of the residue value in phases A, B, C, and the cost function are shown in Fig. 7(a). As it can be seen, the value of the cost function is increased after the fault; the phase A has the highest residue value. Moreover, the current in phase A, cost function, threshold value and fault signal are shown in Fig. 7(b). As it is shown, the fault is detected effectively.

The open phase fault is studied in the next part. Experimental results of this test are shown in Figs. 7(c) and 7(d), respectively. According to the results, proposed FD method is able to detect the open phase fault without using any auxiliary variable.

Finally, the performance of FD method under faulty mode control is considered. A single switch fault is forced in phase *B* of the inverter. The experimental waveforms of this case are shown in Figs. 7(e) and 7(f), respectively. It can be seen from the results that the proposed FD method is able to detect the fault under faulty mode as well.

HERE FIG. 7

In the fourth part, short circuit FD is studied. An upper switch in phase *B* is short circuited. The motor terminal at phase *B* is permanently connected to positive rail of DC-link voltage. Experimental waveforms of the phase currents and the cost function are shown in Fig. 8 at the left side. As it can be seen, after the fault is applied, the phase *B* current is always positive with a high DC value. The residue value in phases *A*, *B*, *C* and fault signal in phase *B* are also shown in the right side of Fig. 8. As it can be seen, the residue value in phase *B* has the highest value after the fault. Its sign is negative as well.

HERE FIG. 8

In order to validate the robustness of the control algorithm to parameter uncertainty, a case study is considered. In the first step, the control method of the motor is set with nominal parameter of the model. After that, the phase resistance is reduced by 50 % and the phase inductance is increased by 50 %. Experimental results of this case study are shown in Fig. 9. As it can be seen, the current waveforms are similar under both ideal and non-ideal parameters. So, the developed control method is robust to parameter uncertainty.

HERE FIG. 9

5.2. Experimental Results of Fault-Tolerant Control

The presented FT and FD method are able to maintain the continuous operation of the drive under faulty mode.

In this section, two faults are forced in phases *A* and *B* of the inverter. In the first step, an open switch fault is introduced in phase *A*. After few cycles, a new fault is forced in phase *B*. The experimental results of this case are shown in Fig. 10. The healthy current waveforms and the cost function are shown at the top of Fig. 10(a). As it can be seen, after the fault is applied, the cost function value is increased

significantly. Following FD, the faulty phase is isolated. At the same time, the control method is reconfigured in one faulty phase mode and two-adjacent faulty phase mode, respectively.

The current waveforms of phases *A* and *B*, the cost function, and the operating code are shown at the Fig. 10(a). As it is shown, the fault is detected during less than half of one cycle.

Finally, the performance of the control method in case of the short circuit fault is studied. For this purpose, an upper switch fault is forced in phase *A* of the inverter. The current waveforms and the cost function in this case are shown at top side of Fig. 10(a). As it can be seen, after FD, the faulty phase is isolated; then, the control method is reconfigured according to the new configuration of the inverter. The residue values and fault signal are shown at the bottom of Fig. 10(b). According to these results, the short circuit fault can be effectively detected and isolated using the proposed FD method.

According to experimental results of the FT control shown in this section, it is possible to maintain the continuous operation of the traction motor drive using the proposed FD and FT control method.

HERE FIG. 10

6. Conclusions

A simplified version of the conventional FCS-MPC is presented in this paper. The control method can be used to maintain the continuous operation of a five-phase BLDC motor under healthy, one faulty phase and two-faulty phase modes. According to the presented analysis, the calculations are significantly reduced while performance similar to the conventional control method is achieved.

A new observer based open transistor and short circuit FD method is presented in this paper as well. This method is simple since extra sensors are not necessary to implement the FD method. Also, it is robust to false alarms in common operational modes of an electric vehicle such as speed transients, load transients, acceleration, and reverse operating mode. FD time is quite short as well. It can detect both single switch and open phase faults without using auxiliary variables. High performance of the proposed FD strategy has been validated with the experimental results under different faulty conditions.

In addition, maintaining the continuous operation of the motor under both open switch and short circuit faults in the VSI has been demonstrated with experimental results of the FTC.

References

[1] H. Wang, M. Liserre, and F. Blaabjerg, "Toward Reliable Power Electronics," *IEEE Ind. Electron. Mag.*, vol. 7, no. 2, pp. 17-26, Jun. 2013.

[2] A. Mohammadpour, and L. Parsa, "Global Fault-Tolerant Control Technique for Multi-Phase Permanent-Magnet Machines," *IEEE Trans. Ind. Appl.*, vol. 51, no. 1, pp. 178-186, Jan. 2015.

[3] F. Mekria, J. F. Charpentiera, E. Semailb, "An efficient control of a series connected two-synchronous motor 5-phase with non-sinusoidal EMF supplied by a single 5-leg VSI: Experimental and theoretical investigations," Electric Power System Research, vol. 92, pp. 11–19, Nov. 2012.

[4] B. Aslan, E. Semail, and J. Legranger, "General Analytical Model of Magnet Average Eddy-Current Volume Losses for Comparison of Multiphase PM Machines With Concentrated Winding," *IEEE Trans. Energy Conv.*, vol. 29, no. 1, pp. 72-83, Mar. 2014.

[5] B. Lu and S. Sharma, "A Literature Review of IGBT Fault Diagnostic and Protection Methods for Power Inverters," *IEEE Trans. Ind. Appl.*, vol. 45, no. 5, pp. 1770–1777, Oct. 2009.

[6] M. Alavi, D. Wang, and M. Luo, "Short-Circuit Fault Diagnosis for Three-Phase Inverters Based on Voltage Space Patterns," *IEEE Trans. Ind. Electron.*, vol. 61, no. 10, pp. 5558-5569, Oct. 2014.

[7] N. M. A. Freire, J. O. Estima, and A. J. M. Cardoso, "A Voltage-Based Approach Without Extra Hardware for Open-Circuit Fault Diagnosis in Closed-Loop PWM AC Regenerative Drives," *IEEE Trans. Ind. Electron.*, vol. 61, no. 9, pp. 4960-4970, Sep. 2014.

[8] A. M. Santos Mendes, M. Bandar Abadi, S. M. A. Cruz, "Fault diagnostic algorithm for three-level neutral point clamped AC motor drives, based on the average current Park's vector," *IET Power Electron.*, 2014, Vol. 7, Iss. 5, pp. 1127–1137

[9] J. Fang, W. Li, H. Li and X. Xu, "On-line Inverter Fault Diagnosis of Buck-Converter BLDC Motor Combinations," *IEEE Trans. Power Electron.*, vol. 30, no. 5, pp. 2674-2688, May. 2015.

[10] P. G. Potamianos, E. D. Mitronikas, and A. N. Safacas, "Open-Circuit Fault Diagnosis for Matrix Converter Drives and Remedial Operation Using Carrier-Based Modulation Methods," *IEEE Trans. Ind. Electron.*, vol. 61, no. 1, pp. 531-545, Jan. 2014.

[11] H. Guzman, F. Barrero, M. J. Duran, "IGBT-Gating Failure Effect on a Fault-Tolerant Predictive Current Controlled 5-Phase Induction Motor Drive," *IEEE Trans. Ind. Electron.*, vol. 62, no. 1, pp. 15-20, Jan. 2015.

[12] Chee Shen Lim, E. Levi, M. Jones, N. Abd. Rahim, and Wooi Ping Hew, "FCS-MPC-Based Current Control of a Five-Phase Induction Motor and its Comparison with PI-PWM Control," *IEEE Trans. Ind. Electron.*, vol. 61, no. 1, pp. 149-163, Jan. 2014.

[13] H. Seng Che, E. Levi, M. Jones, Wooi-Ping Hew, and N. Abd. Rahim, "Current Control Methods for an Asymmetrical Six-Phase Induction Motor Drive," *IEEE Trans. Power Electron.*, vol. 29, no. 1, pp. 407-417, Jan. 2014.

[14] R. S. Arashloo, M. Salehifar, L. Romeral, V. Sala, "Ripple Free Fault Tolerant Control of Five Phase Permanent Magnet Machines," *15th European conference on Power Electronics and Applications (EPE) 2013*, pp. 1-5.

[15] Morel F, Lin-Shi X, Retif J, Allard B, Buttay C., "A comparative study of predictive current control schemes for a permanent-magnet synchronous machine drive," *IEEE Trans. Ind. Electron.*, vol. 56, no. 7, pp. 2715–28, Apr. 2009.

[16] Kenny H, Lorenz D., "Stator- and rotor-flux-based deadbeat direct torque control on induction machines," *IEEE Trans. Ind. Appl.*, vol. 39, no. 4, pp.1093–100, Aug. 2003.

[17] R. S. Arashloo, M. Salehifar, L. Romeral, V. Sala, "A robust predictive current controller for healthy and open-circuit faulty conditions of five-phase BLDC drives applicable for wind generators and electric vehicles," Energy Conversion and Management 92 (2015) 437–447.

[18] J. L. Romeral Martinez, R. Salehi Arashloo, M. Salehifar, J. M. Moreno, "Predictive current control of outer-rotor five-phase BLDC generators applicable for off-shore wind power plants," Electric Power System Research 121 (2015) 260–269.

[19] Wei Chena, Xiujie Genga, Tao Liua, Changliang Xia, "Stationary frame deadbeat power control of three-phase PWM rectifiers under unbalanced grid voltages," Electric Power Systems Research 108 (2014) 223– 233.

[20] J. F. Stumper, V. Hagenmeyer, S. Kuehl, and R. Kennel, *"Deadbeat Control for Electrical Drives: A Robust and Performant Design Based on Differential Flatness," IEEE Trans. Power Electron.*, vol. 30, no. 8, pp. 4585-4596, Aug. 2015.

[21] H. A. Young, M. A. Perez, J. Rodriguez, and H. Abu-Rub, "Assessing Finite-Control-Set Model Predictive Control: A Comparison with a Linear Current Controller in Two-Level Voltage Source Inverters*," IEEE Ind. Electron. Mag.*, vol. 8, no. 1, pp. 44-52, March 2014.

[22] T. Geyer, D. E. Quevedo, "Performance of Multistep Finite Control Set Model Predictive Control for Power Electronics," IEEE Trans. Power Electron., vol. 30, no. 3, pp. 1633 – 1644, Mar. 2015.

[23] M. Salehifar, R. S. Arashloo, M. Moreno-Eguilaz, V. Sala, "Open circuit fault detection based on emerging FCS-MPC in power electronics systems," 15th European Conference on Power Electronics and Applications (EPE), pp. 1 - 10, 2013.

[24] H. Guzman, M. J. Duran, F. Barrero, B. Bogado, and S. Toral, *"Speed Control of Five-Phase Induction Motors With Integrated Open-Phase Fault Operation Using Model-Based Predictive Current Control Techniques," IEEE Trans. Ind. Electron.*, vol. 61, no. 9, pp. 4474-4484, Sep. 2014.

[25] F. Meinguet, E. Semail, J. Gyselinck, "An On-line Method for Stator Fault Detection in Multiphase PMSM Drives," Vehicular Power and propulsion Conference (VPPC), 2010.

[26] V. Yaramasu, M. Rivera, M. Narimani, Bin Wu, and J. Rodriguez, *"Model Predictive Approach for a Simple and Effective Load Voltage Control of Four-Leg Inverter With an Output LC Filter," IEEE Trans. Ind. Electron.*, vol. 61, no. 10, pp. 5259-5270, Oct. 2014.

[27] Changliang Xia, Tao Liu, Tingna Shi, and Zhanfeng Song, "A Simplified Finite-Control-Set Model-Predictive Control for Power Converters," *IEEE Trans. Ind. Inform.*, vol. 10, no. 2, pp. 991-1002, May 2014.

[28] W. Xie, X. Wang, F. Wang, Wei Xu, R. M. Kennel, D. Gerling, and R. D. Lorenz, *"Finite Control Set-Model Predictive Torque Control with a Deadbeat Solution for PMSM Drives," IEEE Trans. Ind. Electron.*, To be published.

[29] M. Rivera, V. Yaramasu, Ana Llor, J. Rodriguez, Bin Wu, and Maurice Fadel, *"Digital Predictive Current Control of a Three-Phase Four-Leg Inverter," IEEE Trans. Ind. Electron.*, vol. 60, no. 11, pp. 4903-4912, Nov. 2013.

[30] O. Lopez, D. Dujic, M. Jones, F. D. Freijedo, J. Doval-Gandoy, and E. Levi, "Multidimensional Two-Level Multiphase Space Vector PWM Algorithm and Its Comparison With Multifrequency Space Vector PWM Method," *IEEE Trans. Ind. Electron.*, vol. 58, no. 2, pp. 465-475, Feb. 2011.

Figure Captions

Fig. 1: The system under study.

Fig. 2: Switching vectors of the five-phase inverter.

Fig. 3: The block diagram of the control method (a) FT control algorithm (b) FD block.

Fig. 4: Reference current, current derivative, and energy of error under different conditions (a) normal operation (b) one faulty phase mode (c) two-adjacent faulty phase (d) two non-adjacent faulty phase.

Fig. 5: Experimental setup.

Fig. 6: Robustness evaluation of FD method to: (a) load transients (at 30 rpm) (b) reverse operation (-30 rpm to 30 rpm) (c) acceleration mode (10 to 50 rpm) (d) deceleration mode (50 to 10 rpm).

Fig. 7: Experimental results of the open switch FD under (a) single switch fault (at 50rpm) (b) open phase fault (c) single switch fault under faulty mode control.

Fig. 8: Experimental results of short circuit FD under upper switch short circuit fault (at 30 rpm).

Fig. 9: Experimental results of controller performance under parameter uncertainty (a) nominal parameters (b) non-ideal parameters (R*0.5 and L*1.5) (at 40 rpm).

Fig. 10: Experimental results of fault-tolerant control (a) healthy phase currents and cost function - faulty phase currents and fault signal (at 30 rpm) (b) experimental waveforms of the short circuit fault (at 50 rpm).

Tables

Table I: faulty switch localization for open switch (oc) and short circuit (sc) fault

S	S_a	S_b	S_c	S_d	S_e	Phase current	sc	oc
S_1	> 0					$i_a=0$		yes
S_2	< 0					$i_a=0$		yes
S_1S_2								yes
S_3		> 0				$i_b=0$		yes
S_4		< 0				$i_b=0$		yes
S_3S_4								yes
S_5			> 0			$i_c=0$		yes
S_6			< 0			$i_c=0$		yes
S_5S_6								yes
S_7				> 0		$i_d=0$		yes
S_8				< 0		$i_d=0$		yes
S_7S_8								yes
S_9					> 0	$i_e=0$		yes
S_{10}					< 0	$i_e=0$		yes
S_9S_{10}								yes
S_1	< 0					$i_a \neq 0$	yes	
S_2	> 0					$i_a \neq 0$	yes	
S_3		< 0				$i_b \neq 0$	yes	
S_4		> 0				$i_b \neq 0$	yes	
S_5			< 0			$i_c \neq 0$	yes	
S_6			> 0			$i_c \neq 0$	yes	
S_7				< 0		$i_d \neq 0$	yes	

S_8				> 0		$i_d \neq 0$	yes	
S_9					< 0	$i_e \neq 0$	yes	
S_{10}					> 0	$i_e \neq 0$	yes	

Table II: Parameters used in control method under ideal and inaccurate conditions

Test Number	Parameter	Parameter uncertainty
1	Ideal condition	Accurate model
2	Inverter nonlinear	$T_{dead\text{-}time}=4$ μs $v_{igbt}(t)=0.018+0.01i(t)$ $v_{diode}(t)=0.018+0.01i(t)$
3	Phase self-resistance	$R_s \times 0.7$
4		$R_s \times 1.3$
5	Phase self-inductance	$L_s \times 0.8$
6		$L_s \times 1.2$
7	Dc-link voltage	$V_{dc} \times 0.8$
8		$V_{dc} \times 1.2$
9	Back EMF	$E \times 0.8$
10		$E \times 1.2$

Table III: Parameters of Five-Phase Motor

Number of Pole Pairs		26
Stator Resistance		0.1 Ω
Stator Inductance	l	408 μH
	m_1	15 μH
	m_2	18 μH
Nominal Torque		8 Nm

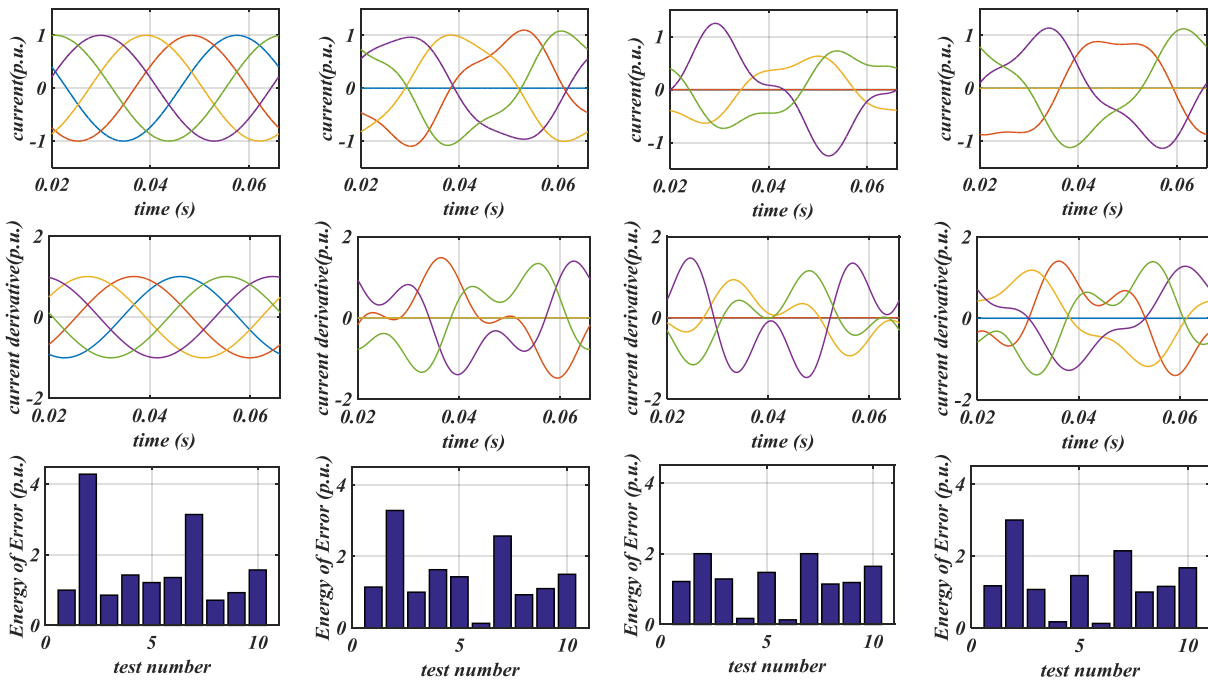| Nominal Speed	400 rpm
Permanent Magnet Flux	0.0178 Wb
Moment of Inertia	0.0583 kgm^2

FIGURES

Fig. 1.

Fig. 2.

(a)

(b)

Fig. 3.

(a)   (b)   (c)   (d)
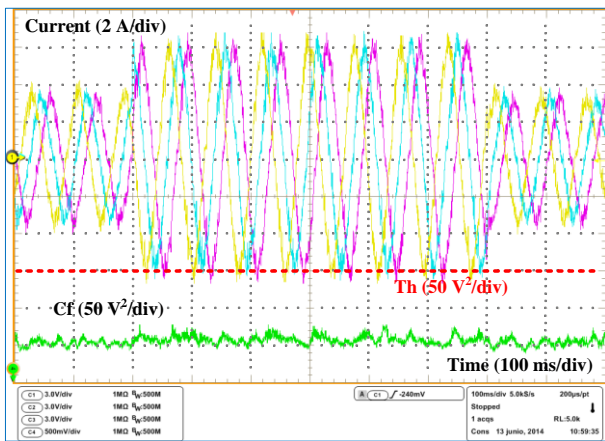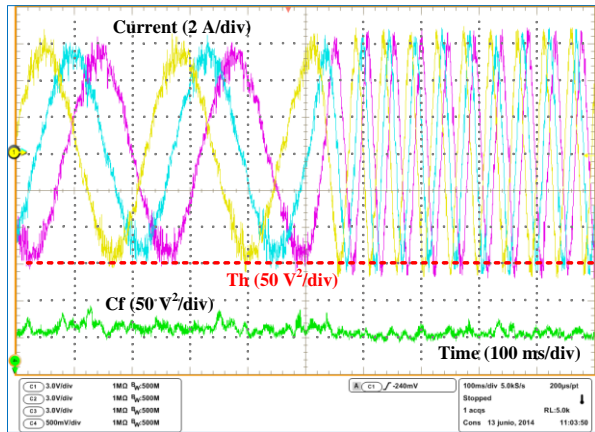
Fig. 4.

Fig. 5.

(a)

(b)
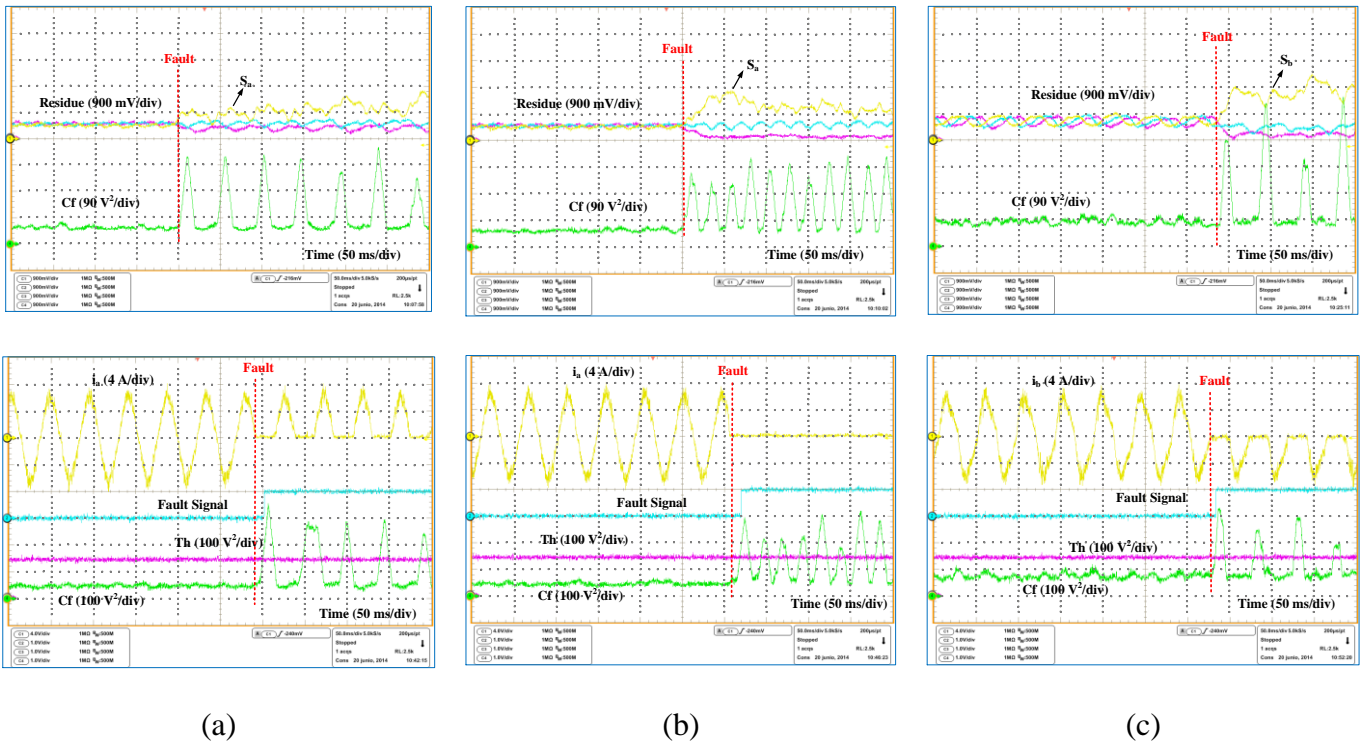

(c)

(d)

Fig. 6.

(a)   (b)   (c)
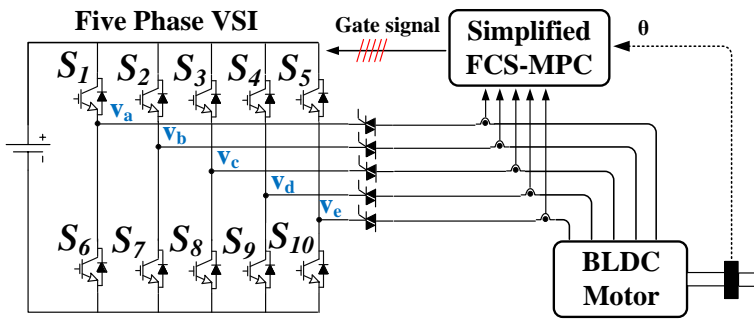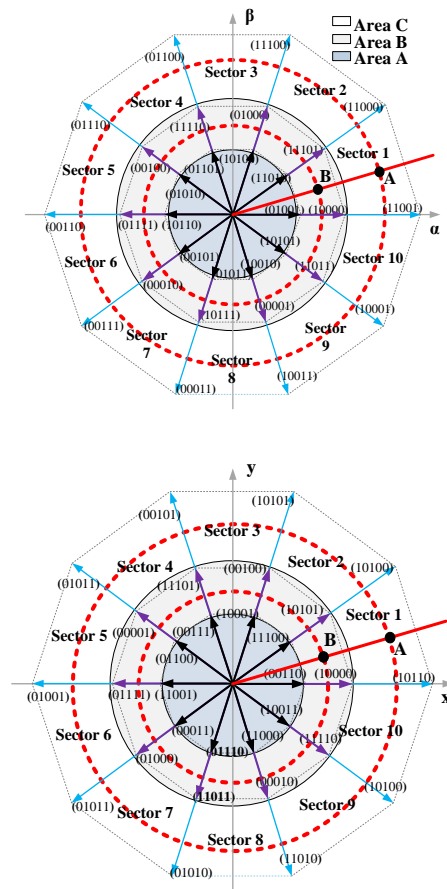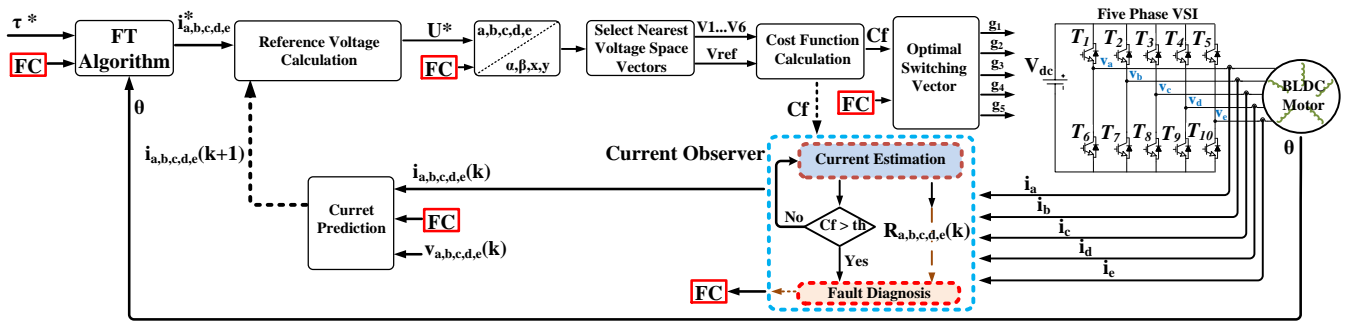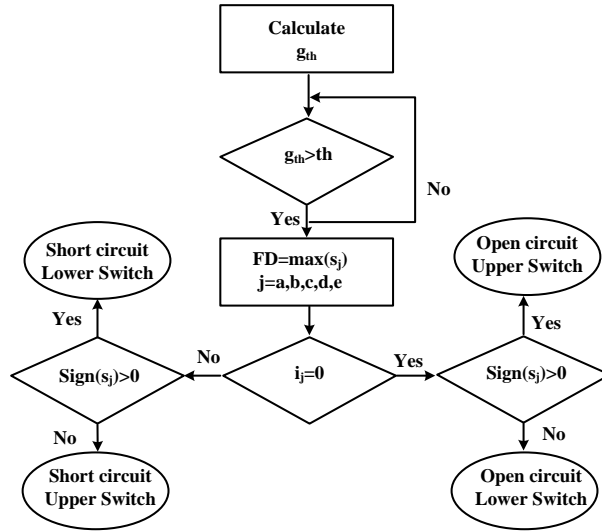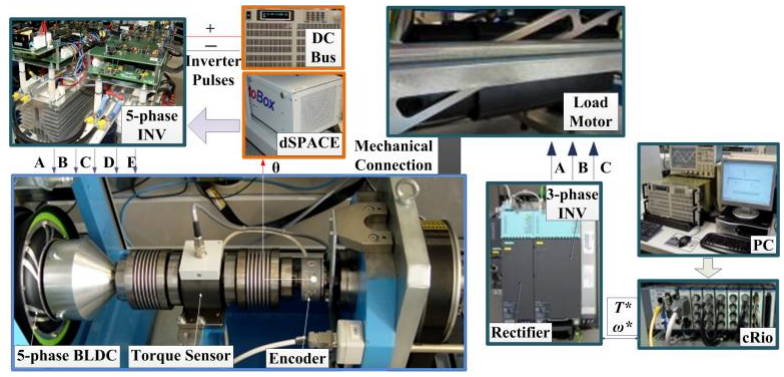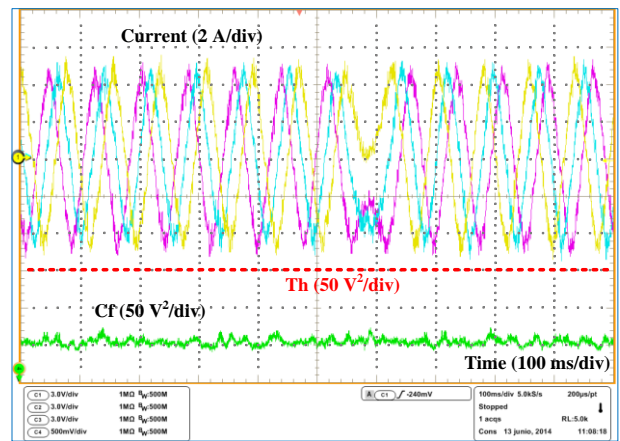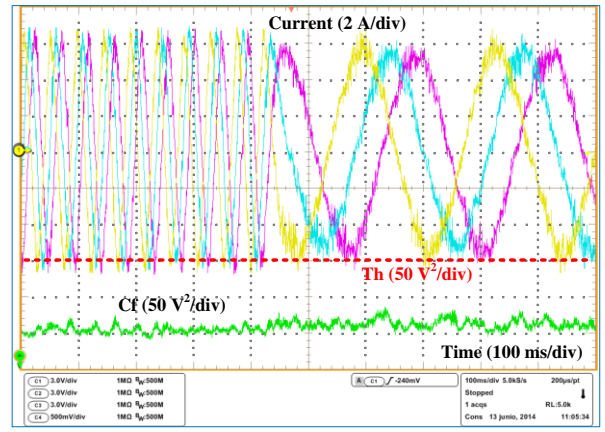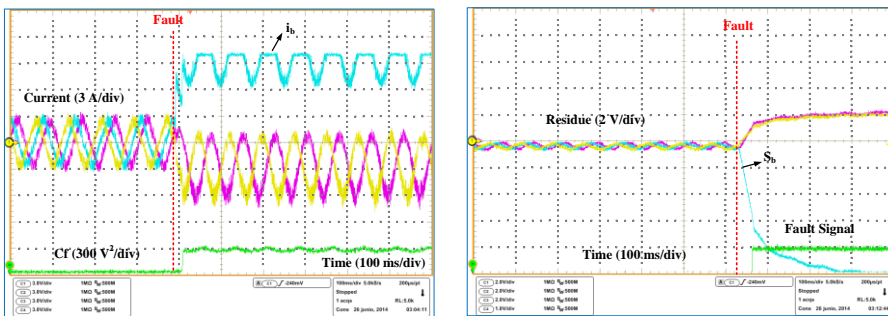
Fig. 7.

Fig. 8.

Fig. 9.

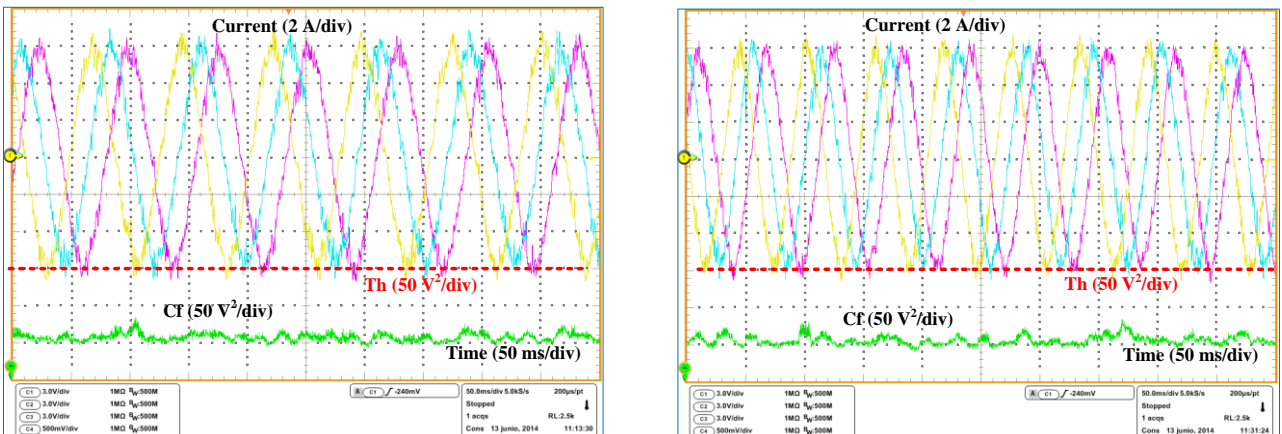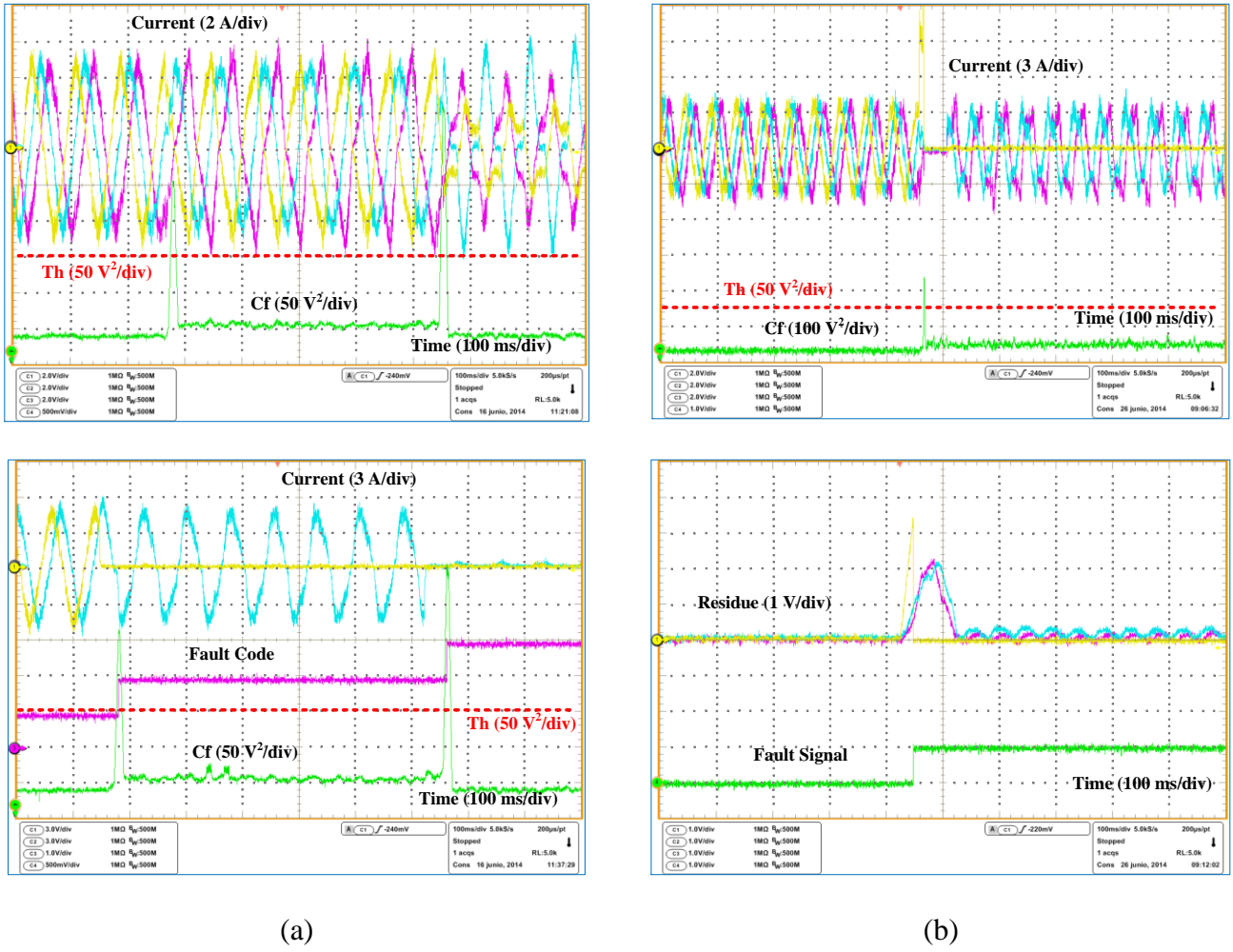
Fig. 10.

(a)   (b)

- A simplified FCS-MPC of a five-phase BLDC motor drive applicable in electric Vehicles has been proposed.

- A FD method has been proposed capable of detection and localization of both open circuit and short circuit faults in voltage source inverter.

- Effect of parameters uncertainty on controller performance has been analysed.

- Theory has been validated with experimental results.

Dear editor,

Thank you very much for agreeing to review the following manuscript:

Manuscript Title: "Simplified Fault Tolerant Finite Control Set Model Predictive Control of a Five-Phase Inverter Supplying PM Motor in Electric Vehicle Drive"

Manuscript Number: EPSR-S-15-00245

We would like to thank the Reviewers, as well as the Associated Editor, for giving us guidance with their helpful comments.

As suggested by the editor, a throughout revision of the paper has been carried out and the comments of the reviewers have been properly answered in the current version of the manuscript. Significant changes made on the original version of the manuscript appear highlighted in color text in the current version. Below you can find the author's response.

Reviewer #1: The paper presents an interesting and useful approach for the diagnosis of faults in a 5-phase BLDC drive.

In spite of that, some improvements can be made, as well as some questions should be clarified.

a) First, the abstract of the paper should be rewritten, making it shorter and, above all, more incisive and more focused on what has been originally presented in the paper.

According to the reviewer comment, the abstract has been modified, the contributions of the paper has been highlighted. Also it has been rephrased to be more incisive. Modifications in the new version of the manuscript are highlighted with <mark>yellow</mark> color.

b) Regarding the types of faults that the diagnostic system is able to detect and isolate, there are short-circuits in the power switches. If a short-circuit happens in one of the IGBTs of a given leg of the inverter, when this faulty switch is turned off and the other switch of the same leg is turned on, won't the current be so high that could lead to the destruction of both IGBTs? How is fault tolerance achieved in this context? Are there in your drive intelligent gate drivers that disable the gate signal of the second IGBT by monitoring the VCE voltage? The authors need to answer these questions in the paper.

Thanks for the comment.

In case of a shoot through in one leg of the inverter, the whole system may shutdown. The main concern under this condition is to detect and isolate the faulty leg. It should be noted that modern gate drives are able to detect this fault. Therefore, the feedback from the gate driver can be sent to the proposed FT control algorithm to isolate the faulty leg and maintain continuous operation of the motor.

In the system under study, Skyper32 gate drivers from Semikron are used to control IGBT switches. Short circuit protection is done by sensing the Collector-Emitter voltage when IGBT is on. Also, the gate driver can be set so that it never allows the second IGBT in the same leg is turned on while other switch is still on. This protection mechanism is so effective to avoid shoot through. In addition, a feedback signal is generated by the gate

driver after short circuit FD. Therefore, the FT controller can isolate the faulty leg and reconfigure the whole drive after receiving the fault feedback from gate driver IC.

Modifications in the new version of the manuscript are highlighted with <mark>yellow</mark> color.

c) Throughout the document, in some parts the authors talk about BLDC drive while in others talk in PM motors. Make it uniform and use solely BLDC drive throughout the document.

Thanks for the reviewer comment.

According to the comment, the BLDC motor has been used throughout the paper; modified sections are highlighted with <mark>yellow</mark> color in the new version of the manuscript.

d) Your topology has a drawback that was not highlighted in the paper: the TRIACs are inserted between the inverter and the motor, meaning that you will have always a small voltage drop across these elements even in healthy conditions. This reduces the maximum voltage that can be applied to the motor, forcing the drive to enter in the field-weakening region a little bit sooner than expected (and this operating mode is important specially in electric vehicles). Highlight this fact in the paper.

As it has been correctly mentioned by reviewer, the voltage drop on TRIACS reduces the maximum voltage available. This design limit should be considered in design of a practical motor drive systems working in field-weakening region.

This limit has been highlighted in new version of the manuscript with <mark>yellow</mark> color.

e) By examining (17) and (18) the reader has some doubts about how open-circuit and short-circuit faults can be distinguished. Also, in Table I, it is not clear what the column "current" contains! Current where? Develop more the process of identification of a short-circuit fault.

Thanks for the reviewer comment.

"Current" means phase current value in faulty phase. In order to distinguish the faulty phase, this simple fact has been used by authors:

Under the short circuit fault, the phase current in faulty phase is increased with an dc component, therefore phase current is non-zero. On the other side, current value is reduced to zero under open switch fault.

To locate faulty switch, the sign of residue in (16) is used to localize the faulty switch. In case of the short circuit fault in an upper switch, sign is positive while under open upper switch fault, the sign is negative.

The block diagram of FD block has been included in the new version of the manuscript as:
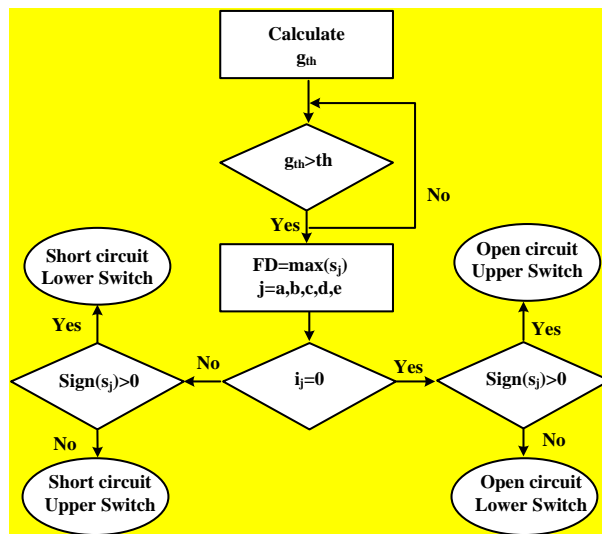
The modifications have been highlighted in the new version of the manuscript with <mark>yellow</mark> color.

Apart from these aspects, the experimental validation is well presented and the results support the claims made in the paper.

Reviewer #3: The work proposes an interesting control and fault diagnostics method. However, some points need to be clarified prior to publication.

1. An English review is required.

Thank you for the comment.

The English of the paper has been thoroughly modified.

Modifications in the new version of the manuscript are highlighted with red text color.

2. The proposed simplification, where the reference voltage is computed based on the solution of the system model and then the nearest voltage space vector is chosen means that this part of the control has a minimum time control (deadbeat) behavior. This has several implications, but these are not discussed in the manuscript. This reviewer's opinion is that the dynamics of the closed loop control can be strongly affected by this. As a deadbeat response is expected, the theoretical influence of model parameter variations needs to be analyzed in depth. This is very important since the machine resistances vary quite a bit depending on the operation temperature.

Thanks for the reviewer's comment.

As it has been truly mentioned, the deadbeat control has been used to predict the motor reference voltages for the next sampling step. This fact has two impacts.

1- Computation delay can affect the performance of the controller and its transient response.

2- Due to use of motor model, controller performance is affected by uncertainty.

The following approach has been used by the authors to address these drawbacks:

Delay Compensation approach:

In practice, performance of a predictive controller is affected by delay due to calculation in digital signal processor, gate drivers, and non-ideal switches [20], [28]. Delay due to

computation time is the most important one among others [28]. This delay can be compensated by calculating the reference voltage so that current at the end of the next sampling period (i.e. i(k+2)) is equal to the reference current. Therefore, it is possible to do the computations during the current sampling period without affecting the controller performance.

Sensitivity Analysis

According to the proposed control method, the machine model in (1) is used to predict the reference voltages similar to predictive deadbeat control method. Therefore, the performance of the simplified FCS-MPC is affected by parameter uncertainties. This issue is analysed in detail in the following. After that, simulation results in Matlab-Simulink are conducted to demonstrate the effect of uncertainties. Results are presented for all operating conditions of the motor drive.

The behaviour of the control method can be affected in different ways. The non-ideal dc link voltage, nonlinear behaviour of the inverter, and inaccuracy in parameters of the motor model are the most important ones among others. Each case is briefly discussed here.

The error in dc-link voltage measurement, the error due to non-linear inverter caused by switching dead time and voltage drop, and error in estimated back EMF can be modelled in (1) as:

$$u(k) = u(k)_{nom} + \Delta u(k)$$

(21)

where Δu(k) is the modelled voltage error and u(k)$_{nom}$ is the ideal input. Since after, all ideal variables are shown with lower case x$_{nom}$.

Similarly, the error in the stator phase resistance and phase self-inductance can be modelled as:

$$A = A_{nom} + \Delta A$$

(22)

$$B = B_{nom} + \Delta B$$

(23)

where ΔA and ΔB are the error in the phase resistance, and self-inductance, respectively.

Current prediction is rewritten in presence of uncertain parameters by replacing (21)-(23) in (8) as follows:

$$x(k+1) = T_{samp} \times ((A + \Delta A)x(k) + Bu(k)) + x(k)$$
$$= x(k+1)_{nom} + \Delta x(k+1) \tag{24}$$

$$x(k+1) = T_{samp} \times (Ax(k) + B(u(k) + \Delta u(k))) + x(k)$$
$$= x(k+1)_{nom} + \Delta x(k+1) \tag{25}$$

$$x(k+1) = T_{samp} \times (Ax(k) + (B + \Delta B)u(k)) + x(k)$$
$$= x(k+1)_{nom} + \Delta x(k+1) \tag{26}$$

By replacing (24)-(26) in (9), the equivalent voltage control under non-ideal condition is calculated as follows:

$$U_{eq} = B^{-1}((x*(k+2) - x(k+1) - \Delta x(k+1)) \times T_{samp}^{-1} - (A + \Delta A)(x(k+1) + \Delta x(k+1)))$$
$$= U_{eq-nom} - T_{samp}^{-1}B^{-1}\Delta x(k+1) \times (1 + T_{samp} \times (A + \Delta A)) - B^{-1}\Delta A x(k+1) \tag{27}$$

$$U_{eq} = (B + \Delta B)^{-1}((x*(k+2) - x(k+1) - \Delta x(k+1)) \times T_{samp}^{-1} - A(x(k+1) + \Delta x(k+1)))$$
$$= U_{eq-nom} - \Delta B / B \times B^{-1}((x*(k+2) - x(k+1)) \times T_{samp}^{-1} - Ax(k+1))$$
$$- T_{samp}^{-1}B^{-1}(1 - \Delta B / B)\Delta x(k+1) \times (1 + T_{samp} \times A) - B^{-1}\Delta A x(k+1) \tag{28}$$

$$U_{eq} = B^{-1}(((x*(k+2) - x(k+1) - \Delta x(k+1))T_{samp}^{-1} - A(x(k+1) + \Delta x(k+1))))$$
$$= U_{eq-nom} - T_{samp}^{-1}B^{-1}\Delta x(k+1) \times (1 + T_{samp} \times A) \tag{29}$$

Equivalent voltages in (27)-(29) can be further simplified as:

$$U_{eq} = U_{eq-nom} - B^{-1}\Delta A(x(k) \times (1 + T_{samp} \times (A + \Delta A)) + \Delta A x(k+1)) \tag{30}$$

$$U_{eq} = U_{eq-nom}(1 - \Delta B / B) - B^{-1}\Delta B(1 - \Delta B / B)u(k) \times (1 + T_{samp} \times A) \tag{31}$$

$$U_{eq} = U_{eq-nom} - \Delta u(k) \times (1 + T_{samp} \times A) \tag{32}$$

As it can be seen in (30)-(32), the non-ideal voltage value can be decreased by reducing the sampling period. On the other side, higher absolute value of parameters and dc-link voltage error can cause a higher error. According to (31), if the error in phase self-inductance is equal to 100 % of real value, controller becomes unstable.

In the following section, simulations are conducted to study the effects of the uncertainty on controller performance. To study the effect of parameter uncertainty, several tests are considered according to table II. For each case, the energy of error is calculated as follows:

$$E = \int (i_a^* - i_a)^2 + (i_b^* - i_b)^2 + (i_c^* - i_c)^2 + (i_d^* - i_d)^2 + (i_e^* - i_e)^2 dt. \tag{33}$$

Under each operating mode, phase current in per-unit, derivative of phase current normalized with respect to the healthy phase current, and energy of the error are calculated. The final results are shown in Fig. 4 under normal, one-faulty phase, two-adjacent faulty phase, and two-non-adjacent faulty phase. According to Fig. 4, inverter non-linear parameters can result in a high error. The inverter non-linearity causes the highest error. Results under two-faulty phase condition are shown in Figs. 4(c) and 4(d), the over-estimation of the self-inductance has a higher impact on accuracy of control method. According to the results, energy of the error under faulty mode in most cases is higher than normal mode operation. According to the current waveforms shown in Fig. 4, symmetrical waveforms and slower dynamics are the main reasons for lower error under normal mode operation.

Table II. Parameters used in control method under ideal and inaccurate conditions

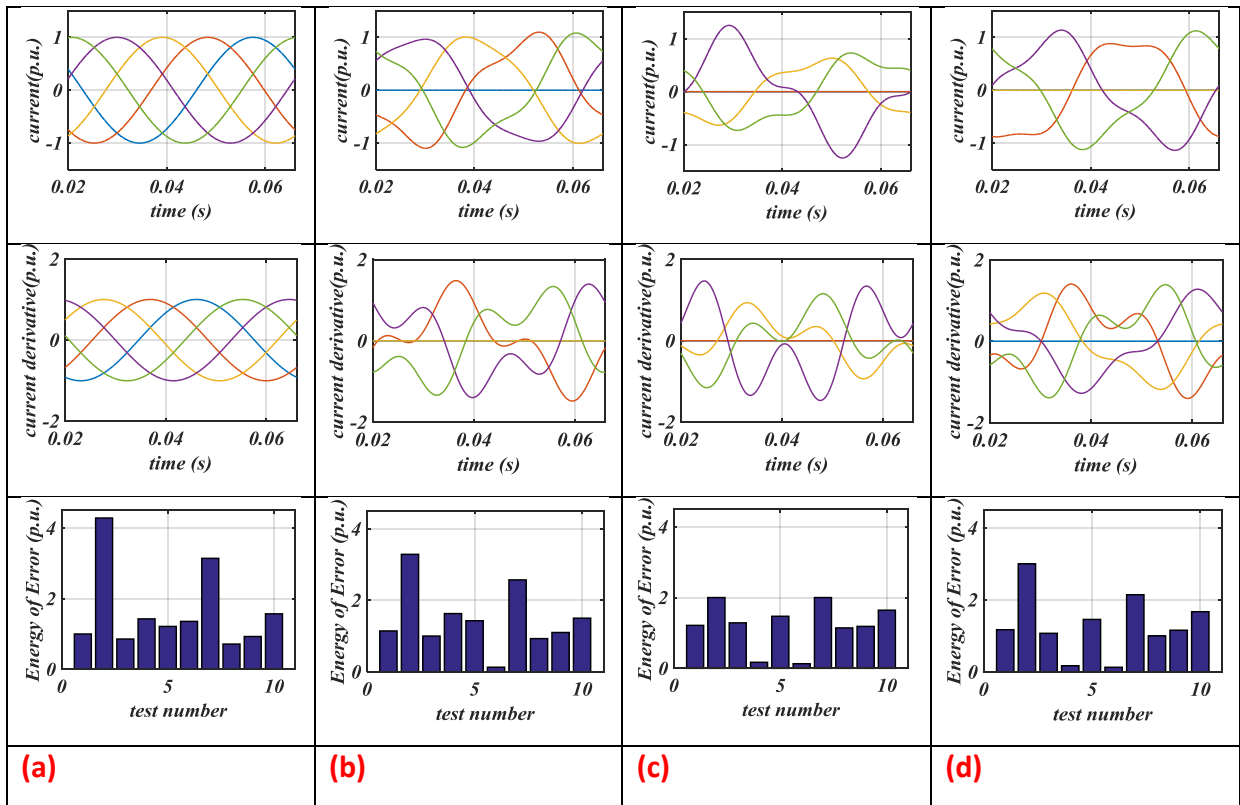| Test Number	Parameter	Parameter uncertainty
1	Ideal Condition	Accurate model
2	Inverter Nonlinear	$T_{dead-time}=4\ \mu s$ $v_{igbt}(t)=0.018+0.01i(t)$ $v_{diode}(t)=0.018+0.01i(t)$
3	Phase self-resistance	$R_s \times 0.7$
4		$R_s \times 1.3$
5	Phase self-inductance	$L_s \times 0.8$
6		$L_s \times 1.2$
7	Dc-link voltage	$V_{dc} \times 0.8$
8		$V_{dc} \times 1.2$
9	Back EMF	$E \times 0.8$
10		$E \times 1.2$

Fig. 4. Reference current, current derivative, and energy of error under different conditions (a) normal operation (b) one faulty phase mode (c) two-adjacent faulty phase (d) two non-adjacent faulty phase.

Modifications are highlighted with blue color in the new version of the manuscript.

3. A brief review on deadbeat control methods would be interesting to the reader.

According to the reviewer comment, a brief review was done on deadbeat control in new version of the manuscript as following.

MPC methods presented in literature can be categorized in two categories: deadbeat control, and FCS-MPC [23]. Regarding deadbeat control method, machine's model is used

to calculate the machines terminal voltages so that motor phase current is able to follow reference current [24], [26]. Predictive deadbeat control is used in [27] to implement the fault-tolerant control of a five-phase BLDC machine under healthy and faulty conditions; a sensitivity analysis has been done on the control method. An improved predictive deadbeat control of five-phase BLDC machine has been presented in [23]; in contrast to presented method in [27], authors use extended Kalman filter to predict the motor phase currents; main advantage is that it can compensate the nonlinearly of the inverter, and error due non-ideal motor parameters. This method has a high computational cost. A deadbeat power control method is presented in [29] to improve steady-state and transient response of PWM rectifier under unbalanced grid conditions. To further improve the controller performance, calculation delay is compensated. A new deadbeat controller based on feedback and feed forward linearization is presented in [28]; this method has a high dynamic response, at the same time it is robust to parameter uncertainties and disturbances.

[24] Morel F, Lin-Shi X, Retif J, Allard B, Buttay C., "A comparative study of predictive current control schemes for a permanent-magnet synchronous machine drive," IEEE Trans. Ind. Electron., vol. 56, no. 7, pp. 2715–28, Apr. 2009.

[26] Kenny H, Lorenz D., "Stator- and rotor-flux-based deadbeat direct torque control on induction machines," IEEE Trans. Ind. Appl., vol. 39, no. 4, pp.1093–100, Aug. 2003.

[27] R. S. Arashloo, M. Salehifar, L. Romeral, V. Sala, "A robust predictive current controller for healthy and open-circuit faulty conditions of five-phase BLDC drives applicable for wind generators and electric vehicles," Energy Conversion and Management 92 (2015) 437–447.

[28] Jean-Francois Stumper, Veit Hagenmeyer, Sascha Kuehl, and Ralph Kennel, "Deadbeat Control for Electrical Drives: A Robust and Performant Design Based on Differential Flatness," IEEE Trans. Power Electron., vol. 30, no. 8, pp. 4585-4596, Aug 2015.

[29] Wei Chena, Xiujie Genga, Tao Liua, Changliang Xia, "Stationary frame deadbeat power control of three-phase PWM rectifiers under unbalanced grid voltages," Electric Power Systems Research 108 (2014) 223– 233.

Modifications in the new version of the manuscript have been highlighted with blue color.

4. The figures do not have captions and, thus, it is difficult to understand some aspects.

Thanks for the comment.

The figure captions are at the end of the reference sections. The captions have been modified to be more informative.

Modifications are highlighted with blue color.

5. There are faults where the semiconductors are neither open or shorted for some time. Would this be a problem for the proposed algorithm?

Thank you for the comment.

Authors believe that output phase current under this mode is zero while the reference current is none zero, this can lead to a false alarm, therefore the proposed FD method identify this case as an open switch fault. If this condition is too short, proposed FD method is still robust to the false alarm.

Since proposed method is not able to identify this state, additional hardware based methods can be used to effectively manage this condition.

This case has been mentioned in the new version of the manuscript. New modifications are highlighted with blue color.